Sensors and Materials, Vol. 31, No. 1 (2019) 53–61
MYU Tokyo

S & M 1747

Surfactant Sensor Based on Waveguide-mode Sensor with Hydrophobic Perforated Surface

Makoto Fujimaki* and Hiroki Ashiba

Electronics and Photonics Research Institute,
National Institute of Advanced Industrial Science and Technology (AIST),
1-1-1 Higashi, Tsukuba, Ibaraki 305-8565, Japan

(Received June 30, 2018; accepted August 20, 2018)

Keywords: optical sensor, water examination, surfactant, nanopore, waveguide-mode resonance

The sensitivity of a waveguide-mode sensor, which has a sensing plate incorporating a thin single-crystalline Si layer and a thin SiO_2 glass layer on a silica glass substrate, can be improved by increasing the surface area of the thin SiO_2 glass layer by forming nanopores. In this study, we achieved the highly sensitive detection of surfactants in water by hydrophobic treatment of the surface of the sensing plate on which nanopores were formed. The hydrophobic treatment ensures that no water enters the nanopores, even when the sensing plate surface is immersed. When a surfactant is present in the water, the surfactant is gradually adsorbed on the sensing plate surface, which leads to hydrophilization; the water can then enter the nanopores. This results in a large refractive index variation on the chip surface, which makes it possible to detect the surfactant with high sensitivity. 0.02 mg/l Tween 20, which is a nonionic surfactant, and 0.02 mg/l sodium dodecyl sulfate, which is an anionic surfactant, were successfully detected using this sensor.

1. Introduction

Surfactants are widely used in manufacturing plants and in homes as synthetic detergents. Rivers, lakes, and marshes are contaminated when effluent that contains surfactants is released into the environment. The Water Quality Standard of the Water Supply Law of Japan stipulates that the concentration of anionic surfactants must be 0.2 mg/l or less and that of nonionic surfactants must be 0.02 mg/l or less. Agricultural chemicals include surfactants that are discharged into the environment when such chemicals are sprayed. The screening test for surfactants in rivers, lakes, and marshes of agricultural areas can serve as an effective means of detecting potential agricultural chemical contamination. Although the evaluation of water can be easily conducted in a laboratory, such a process is not economical because transporting water to a laboratory from the field is time-consuming and expensive. Thus, a method for easily conducting an on-site screening test to determine the level of contamination is desired.

*Corresponding author: e-mail: m-fujimaki@aist.go.jp
https://doi.org/10.18494/SAM.2019.2043

ISSN 0914-4935

Methylene blue absorption spectrophotometry, ethyl violet absorption spectrophotometry, and solvent extraction-flame atomic absorption spectrophotometry, which are currently recognized as official methods of analysis in Japan, are measurement methods that can be used to detect anionic surfactants in environmental water.[1] Tetrathiocyanatocobaltate (II) absorption spectrophotometry and thiocyanate (III) absorption spectrophotometry can be used as measurement methods for nonionic surfactants.[1] However, these are not suitable for on-site detection, because solvent extraction is required for all of these methods, which complicates their analysis procedures and requires a large amount of organic solvent. Methods of detecting and identifying surfactants using high-performance liquid chromatography and mass spectrometry have been developed in recent years, but these methods require large analyzers, which limits their application on site.

In this paper, we report a sensor we developed that can be used as a surfactant screening test device simply by dripping a small amount of water specimen on the sensing plate. This surfactant sensor was developed on the basis of waveguide-mode sensor technology.[2–6] The sensing plate of a waveguide-mode sensor incorporates a thin single-crystalline Si layer and a thin SiO_2 glass layer on a silica glass substrate. It has been reported that the sensor sensitivity can be improved by forming nanopores on the thin SiO_2 layer.[2,3] A perforated waveguide-mode sensor was used for this development.

2. Materials and Methods

EVA-001 (Optex) was used as the waveguide-mode sensor. EVA-001 is a parallel-incidence-type waveguide-mode sensor with a spectral-readout setup.[6] The optical setup of the sensor is shown in Fig. 1. The bottom angle of the prism of the system is 38°. The incident light is converted into s-polarized light by a polarizer and irradiated onto the prism.

A sensing plate with a single-crystalline Si layer and a SiO_2 glass layer thermally grown on a 1.2-mm-thick silica glass substrate was used in the experiments. The sensing plates were cut into smaller plates measuring 18 × 14 mm^2. A silicon-on-quartz (SOQ) substrate (Shin-Etsu Chemical) with a single-crystalline Si layer on a silica glass substrate was used in fabricating

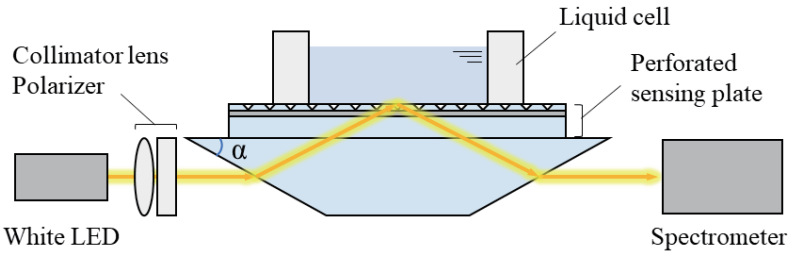

Fig. 1. (Color online) Schematic diagram of the optical setup of waveguide-mode sensor. A water specimen is placed on the sensing plate. An index-matching liquid is placed between the sensing plate and the prism. α: bottom angle of the prism.

this sensing plate. The SiO_2 glass layer was formed by thermally oxidizing the surface of the single-crystalline Si layer of the SOQ substrate.[2] The thicknesses of Si and SiO_2 glass layers evaluated by the manufacturer were 45 ± 2 and 530 ± 5 nm, respectively.

The perforation of the SiO_2 glass layer was conducted by the selective etching of latent tracks created by swift heavy-ion irradiation.[2,3,5] The ion irradiation was performed using the beam line L2 of the 20 MV tandem accelerator at JAEA-Tokai. The ions used were 200 MeV Xe ions that were irradiated onto the sensing plate at room temperature in vacuum of about 5×10^{-4} Pa. The total fluence of the ions was 5×10^{9} cm^{-2}. For etching, the irradiated plates were immersed in 5% hydrofluoric acid solution (Wako Pure Chemical) at room temperature. The etching time interval was adjusted so that the resonance dip, which is observed with the waveguide-mode sensor, was positioned between 600 and 610 nm when ultrapure water was placed on the sensing plate. The time required for etching was approximately 150 s. A 5% solution of dimethyldichlorosilane (DMDCS) in toluene (Sigma-Aldrich) was used for the hydrophobic treatment of the sensing plate. A small amount (150 μl) of toluene solution with 5% DMDCS content was placed in a petri dish of 10 cm diameter. The sensing plate was placed inside the petri dish while ensuring that the surface on which the nanopores were formed was not immersed in the toluene solution. A lid was placed over the petri dish and the hydrophobization of the plate surface was performed by exposing it to DMDCS vapor at 4 °C for 10 min.

A scanning electron microscopy (SEM; JSM-6340F, JEOL) system was used to observe the formed nanopores. The contact angle of the sensing plate surface before and after the hydrophobic treatment was measured using a contact angle gauge (DM-501, Kyowa Interface Science). The volume of the water drop used for contact angle measurement was set to 1 μl.

Polyoxyethylene sorbitan monolaurate (Tween 20; Tokyo Chemical Industry), which is a nonionic surfactant, and sodium dodecyl sulfate (SDS; Wako Pure Chemical), which is an anionic surfactant, were used as the surfactants targeted for detection. These surfactants were diluted with ultrapure water and used as the water specimen. The amount of the water specimen used for each measurement was set to 150 μl. The water specimen was measured by applying it onto the sensing plate.

3. Experimental Results

SEM images of the top and cross-sectional views of the sensing plate with nanopores formed are respectively shown in Figs. 2(a) and 2(b). The diameter of the nanopores, as evident in these figures, was approximately 80 nm on the surface of the chip. The nanopores were conical and had a depth of approximately 180 nm. The thickness of the SiO_2 glass layer was approximately 450 nm. The density of the nanopores actually formed on the sensing plate was derived as 4.5×10^{9} cm^{-2} by counting nanopores on the SEM images.

The solid and broken lines in Fig. 3 indicate the spectra of the ultrapure water measured using the sensing plate before and after the hydrophobic treatment, respectively. A resonance dip was observed at 605 nm for the sensing plate prior to the hydrophobic treatment. The dip position moved to 558 nm after the hydrophobic treatment was performed. This indicated that the refractive index on the plate surface decreased as a result of the hydrophobic treatment.

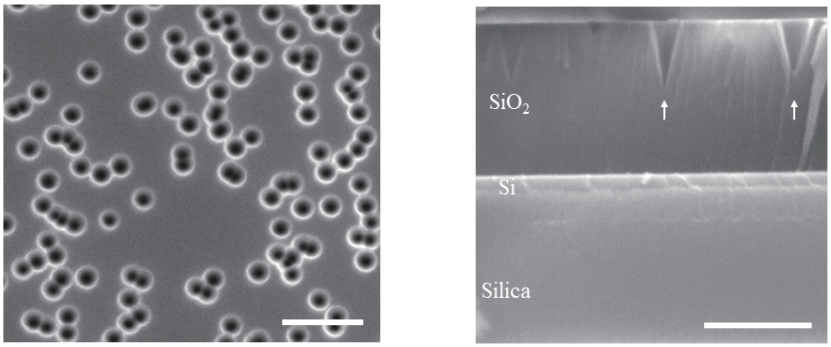

(a) (b)

Fig. 2. SEM images of waveguide-mode sensing plate with nanopores. Scale bars indicate 300 nm. (a) Top view. (b) Cross-sectional view. White arrows indicate nanopores.

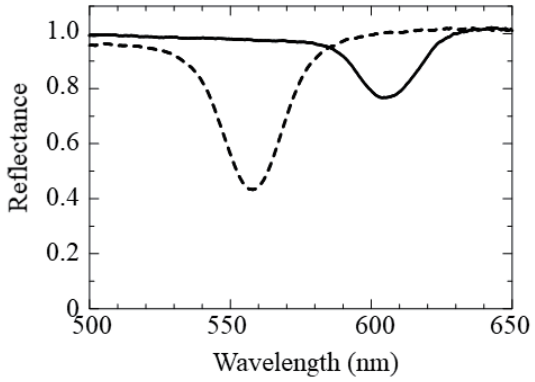

Fig. 3. Reflectance spectra of the perforated sensing plate before (solid line) and after (broken line) hydrophobic treatment. The spectra were measured with ultrapure water on the sensing plates.

The contact angles were measured on the sensing plate surface before and after the hydrophobic treatment. The contact angles for ultrapure water were 14.3 ± 1.4° before the hydrophobic treatment and 110.4 ± 0.7° after the hydrophobic treatment. The hydrophobization of the sensing plate surface by the hydrophobic treatment can also be confirmed from the contact angle measurements.

Figure 4 shows the change in the spectrum when the measurement of the water specimen containing 0.1 mg/l Tween 20 was taken. Solid and broken lines respectively represent the spectra immediately after and 10 min after the water specimen was placed on the sensing plate. It is evident from the figure that the resonance dip shifted to the longer wavelength side. Figure 5 shows the relationship between the elapsed time after the water specimen was applied onto the sensing plate and the amount of change in the position of the resonance dip, where the water specimen contained 0, 0.02, 0.05, 0.1, and 1 mg/l Tween 20. The resonance dip position started to shift towards the longer wavelength side immediately after the water specimen was applied when the water specimen contained Tween 20, and the amount of change became greater with time. Figure 6 shows the relationship between the concentration of Tween 20 and

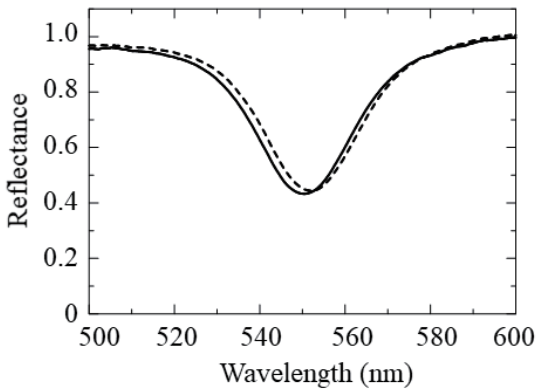

Fig. 4. Reflectance spectra of the perforated sensing plate measured with the water specimen containing 0.1 mg/l of Tween 20. Solid line: immediately after applying water specimen. Broken line: 10 min after applying water specimen.

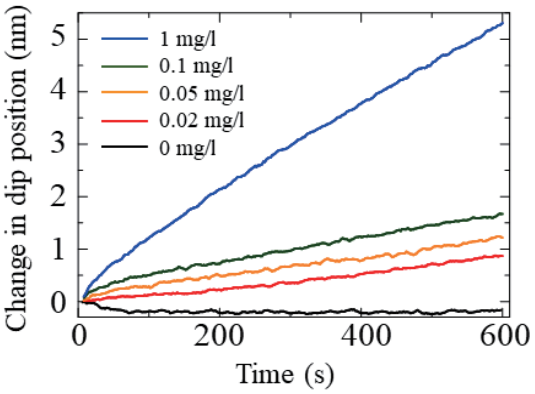

Fig. 5. (Color online) Amount of change in the resonance dip position against time after applying the water specimen containing Tween 20.

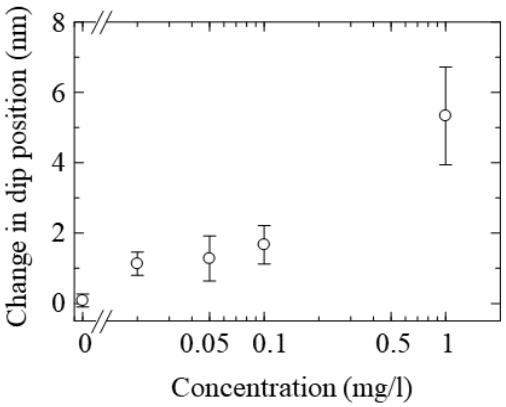

Fig. 6. Amount of change in the resonance dip position 10 min after water specimen injection against concentration of Tween 20.

the amount of change in resonance dip position 10 min after the water specimen was applied. The indicated values were averages of five measurements taken for respective concentrations, and the error bar indicates the standard deviation. Although the error bar is large, it is still evident that the amount of change becomes greater as the concentration of Tween 20 increases.

A similar test was also conducted using SDS as the surfactant. Figure 7 shows the relationship between the time after the water specimen was applied onto the sensing plate and the amount of change in the position of the resonance dip, where the water specimen contained 0, 0.02, 0.2, and 1 mg/l SDS. A shift in dip position was observed in this instance as well. The specimen water with high SDS concentration was also measured. The solid line in Fig. 8 represents the spectrum for the measurement of ultrapure water, and the broken line in Fig. 8 represents the spectrum of the water specimen containing 50 mg/l SDS taken 10 min after water specimen application. The spectrum after 10 min shifted to almost the same position as the spectrum before the hydrophobic treatment shown in Fig. 3.

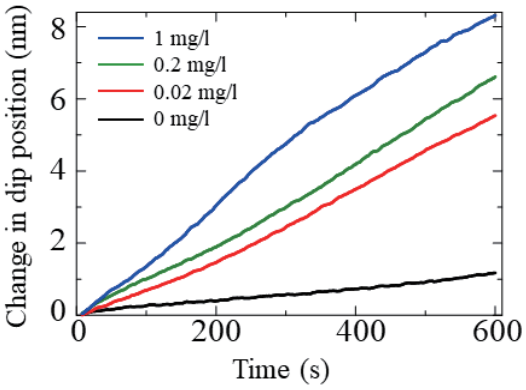

Fig. 7. (Color online) Amount of change in resonance dip position against time after injecting the water specimen containing SDS.

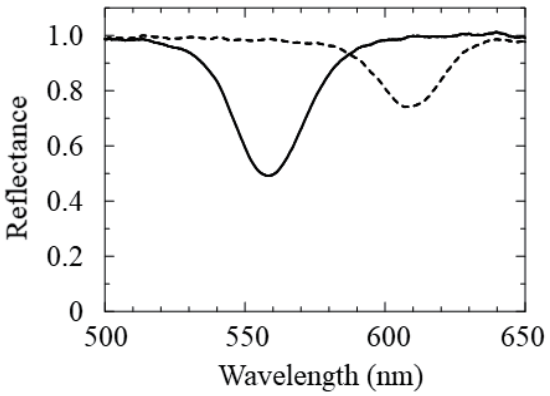

Fig. 8. Reflectance spectra of the perforated sensing plate measured with the water specimen containing 50 mg/l SDS. Solid line: immediately after applying ultrapure water. Broken line: 10 min after applying water specimen.

4. Discussion

The results reveal that the detection of Tween 20 and SDS is possible at the concentrations permitted under the Water Quality Standard as stipulated by the Water Supply Law of Japan, 0.02 and 0.2 mg/l, respectively, using the waveguide-mode sensor with the hydrophobically treated perforated sensing plate. No extraction work or chemicals were required, and the detection was completed within 10 min simply by applying the water specimen onto the sensing plate. The reason why such highly sensitive and rapid detection was possible is considered to be the signal amplification by water.

As shown in Fig. 3, the resonance dip position blue-shifted by approximately 50 nm after the hydrophobic treatment of the sensing plate surface. Formation of a layer of organic substances on a sensing plate surface generally results in the red shift of the resonance dip, because the refractive indices of the organic substances are greater than that of water. The large blue shift indicates that there is a significant reduction in refractive index on the plate surface. Such changes are therefore believed to have occurred not because of the formation of the DMDCS layer on the surface, but because of the water that could no longer penetrate the nanopores owing to the hydrophobic treatment, resulting in a decreased refractive index on the surface of the sensing plate.

The following calculation was performed to prove this idea. The thickness of the SiO_2 glass layer of the sensing plate after etching was approximately 450 nm, as seen in Fig. 2, and the nanopores were conical and had a diameter of 80 and a depth of 180 nm. The model shown in Fig. 9(a) was used for the calculation. For simplicity, the nanopores of the model were approximated as cylinders with a diameter of 80 and a depth of 60 nm. Although the depths of the pores differed from those of the actual sensing plate, the volume was identical. The nanopore density was 4.5×10^9 cm^{-2}, which was derived from the SEM images as described above. We assumed that the nanopores do not overlap each other. The calculation was

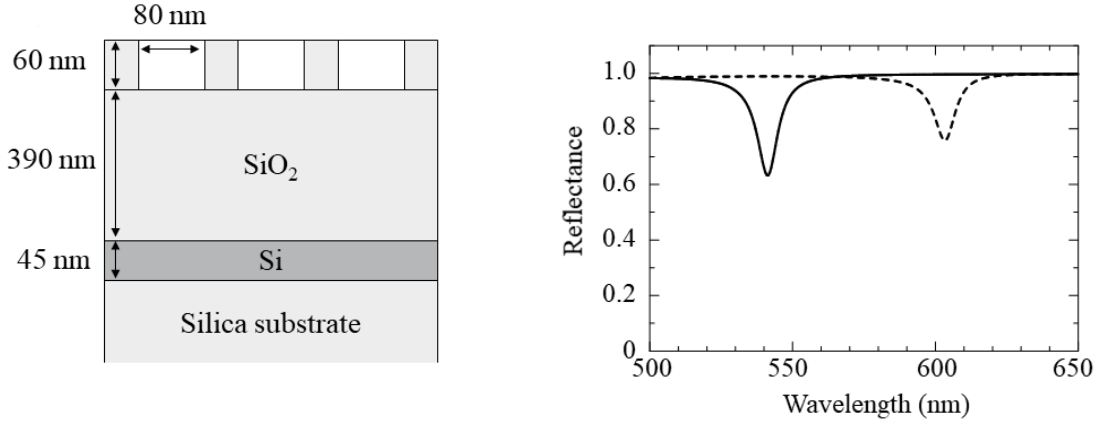

(a) (b)

Fig. 9. Electric field calculation of the perforated sensing plate. (a) Calculation model. (b) Calculated reflectance spectra. The nanopore interior is considered to be air (solid line) and water (broken line).

performed using the transfer matrix method for a stratified medium, in accordance with Fresnel equations.[7] As shown in Fig. 9(a), four layers, namely, the silica glass substrate, the Si layer of 45 nm thickness, the SiO_2 glass layer of 390 nm thickness, and the layer of 60 nm thickness on which the nanopores are formed, were assumed for the calculation. The complex refractive indices of SiO_2 glass,[8] water,[8] and single-crystalline Si[9] used for the calculation were taken from previous reports. In the perforated layer, the nanopore size is small compared with the wavelength of the incident light, and the electric field direction of the light is perpendicular to the axis of the nanopore cylinders. In this case, the effective refractive index of the perforated layer, n_{pg}, can be estimated as[10]

$$1/n_{pg}^2 = \left(1 - f_p\right)/n_g^2 + f_p/n_p^2, \tag{1}$$

where n_g and n_p are the refractive indices of SiO_2 glass and substances in the nanopores, respectively, and f_p is the volume fraction of the nanopores. The calculation was performed with incident s-polarized light and a half-cylindrical prism made of silica glass; the angle of incidence was 70.7°. This angle of incidence was equivalent to that of the incident light in the proximity of wavelength of 600 nm with the optical system shown in Fig. 1.

The reflectance spectrum derived by the calculation is shown in Fig. 9(b). The solid and broken lines in the figure represent the spectra derived by calculation considering the nanopore interior to be air and water, respectively. The resonance dip positions were 541 nm for air and 603 nm for water. These dip positions matched the experimental results shown in Fig. 3. Accordingly, air, not water, is considered to have existed in the interior of the nanopores after hydrophobic treatment. The reason why such highly sensitive detection of the surfactant was possible is concluded to be the significant shift of the dip position owing to the water entering the nanopores, because the hydrophilization of the surface of the nanopores occurred in association with the adsorption of the surfactant on the surface.

The discussion above presupposed that water can enter the nanopores. However, it is not obvious whether water can enter the nanopores of 80 nm diameter. The wettability of a nanoporous surface has been investigated in previous studies using porous anodic alumina.[11,12] In those studies, for example, Ran *et al*. observed that water entered nanopores of 85 nm diameter and 4.5 μm depth while expelling air from the pores.[11] The observations in previous studies, in addition to the matching of resonance dip positions of the measured and calculated reflectance spectra [Figs. 3 and 9(b)], support the assumption that water enters nanopores.

A comparison of the calculated values of the reflection spectrum shown in Fig. 9(b) and the actual measurement values shown in Fig. 3 reveals that the actual measurement values had a broader dip. This phenomenon has been reported and is believed to occur when the surface of the chip is not an ideal flat surface. The dip width is considered to become greater than the calculated value when the nanopores are formed and the surface becomes rough. Previous studies also revealed that the resonance dip becomes shallower than the calculated value with sensing plates that have nanopores.[2] The cause of this is, in the same way, that the plate surface no longer remains flat because of the formation of nanopores. In this study, however, the experimental dip was deeper than the calculated dip as shown in Figs. 3 and 9(b). This phenomenon is particularly significant when air is present inside the nanopores. The reason for the deepened resonance dip is considered to be the scattering of light by the nanopores. Because the difference in refraction index between SiO_2 glass and air is large, the scattering is greater when the nanopores are filled with air than in cases where the nanopores are filled with water. The loss of light is increased as a result, leading to a deeper dip.

In principle, the detection of all surfactants is possible with the developed sensor. Although specific types of surfactants cannot be identified, this sensor is effective for on-site screening to determine the level of contamination by surfactants. Sensitivity to other surfactants and the range in which the sensor is applicable must be verified in future works. Investigations into substances other than surfactants, with which false-positive reactions may occur, are also vital for practical implementation. The presence of alcoholic substances, for instance, may potentially trigger false-positive detections. As a matter of fact, a dip position shift of about 10 nm has been observed with water containing 1% ethanol (data not shown). Although such a high concentration of alcohol being included in environmental water is probably quite rare, it would be necessary to list substances that interfere with measurements.

5. Conclusions

A surfactant sensor was configured by hydrophobic treatment of the surface of a waveguide-mode sensing plate with nanopores. Detection at concentrations specified in the Water Quality Standard in Japan was successful for Tween 20, a nonionic surfactant, as well as for SDS, an anionic surfactant. The factor that made it possible to achieve such a high sensitivity was signal amplification by water. Sensor signals were obtained when the surfactant was adsorbed on the hydrophobic nanopore surface, which resulted in water entering the nanopores. The sensitivity could be explained without any contradiction through a consideration based on calculation. Although it is not possible to identify specific types of surfactants with this method, it is a

promising method that can be adopted as a primary screening technology implemented on site, because detection is possible without the need for any pretreatment or reagents and with a measurement time of less than 10 min.

Acknowledgments

The authors thank the Advanced Functional Materials Research Center of Shin-Etsu Chemical Co., Ltd., for supplying the sensing plate.

References

1 Japan Industrial Standards: JIS K 0102:2013: Testing methods for industrial wastewater.
2 M. Fujimaki, C. Rockstuhl, X. Wang, K. Awazu, J. Tominaga, Y. Koganezawa, Y. Ohki, and T. Komatsubara: Opt. Express **16** (2008) 6408. https://doi.org/10.1364/OE.16.006408
3 K. Awazu, C. Rockstuhl, M. Fujimaki, N. Fukuda, J. Tominaga, T. Komatsubara, T. Ikeda, and Y. Ohki: Opt. Express **15** (2007) 2592. https://doi.org/10.1364/OE.15.002592
4 M. Fujimaki, K. Nomura, K. Sato, T. Kato, S. C. B. Gopinath, X. Wang, K. Awazu, and Y. Ohki: Opt. Express **18** (2010) 15732. https://doi.org/10.1364/OE.18.015732
5 K. Nomura, M. Fujimaki, K. Awazu, and T. Komatsubara: J. Vac. Sci. Technol. A **29** (2011) 051402. https://doi.org/10.1116/1.3609795
6 M. Fujimaki, X. Wang, T. Kato, K. Awazu, and Y. Ohki: Opt. Express **23** (2015) 10925. https://doi.org/10.1364/OE.23.010925
7 M. Born and E. Wolf: Principles of Optics: Electromagnetic Theory of Propagation, Interference and Diffraction of Light (Pergamon, Oxford, 1980) 6th ed.
8 E. Palik and G. Ghosh: Handbook of Optical Constants of Solids (Academic, Cambridge, 1998).
9 G. E. Jellison, Jr.: Opt. Mater. **1** (1992) 41. https://doi.org/10.1016/0925-3467(92)90015-F
10 D.E. Aspnes: Thin Solid Films **89** (1982) 249. https://doi.org/10.1016/0040-6090(82)90590-9
11 C. Ran, G. Ding, W. Liu, Y. Deng, and W. Hou: Langmuir **24** (2008) 9952. https://doi.org/10.1021/la801461j
12 R. Redón, A. Vázquez-Olmos, M. E. Mata-Zamora, A. Ordóñez-Medrano, F. Rivera-Torres, and J. M. Saniger: J. Colloid Interface Sci. **287** (2005) 664. https://doi.org/10.1016/j.jcis.2005.02.036